Formation of Fibril Structures in Polymerizable, Rod–Coil-Oligomer-Modified Epoxy Networks

Yingfeng Yu,*[a] Zongyong Gao,[a] Guozhu Zhan,[a] Liang Li,[a] Shanjun Li,*[a] Wenjun Gan,[b] and James V. Crivello[c]

Abstract: This paper describes the in situ preparation of fibrils in epoxy networks in which the fibril-like structures are cured polymerizable rod–coil oligomers. The epoxy-terminated α,ω-modified PEO oligomers, which are ABA rod–coil–rod oligomers with a poly(ethylene oxide) coil unit and two aromatic azomethine liquid-crystalline rod units, were synthesized and then further blended with an epoxy precursor. Uniform nanoscale columnar structures were observed in the neat rod–

Keywords: epoxy networks · liquid crystals · nanostructures · rod–coil oligomers · self-assembly

coil oligomers as well as in the cross-linked liquid-crystalline state. During the curing of the blends, the supra-molecular nanoscale columnar structures of the rod–coil oligomers are transformed into polymeric fibrils where the epoxy functional end groups have co-reacted with epoxy precursors to form a crosslinked network.

Introduction

Thermosetting networks tend to have a characteristic low resistance to brittle fracture, therefore the modification of these materials with rubbers,[1] thermoplastics,[2] and core–shell particles[3] has been a significant challenge in the past few decades. These modifiers are initially miscible with the uncured thermoset precursors but phase-separate to typically form spherical structures or bicontinuous structures, which means that morphological control is a common chal-lenge in these methods. Furthermore, these methods also have some drawbacks in terms of either thermal, processing, or internal-stress properties. For example, rubber modifica-tion is invariably accompanied by a significant drop in heat resistance, while thermoplastic and core–shell particle addi-tives are usually difficult to disperse in precursors and always sharply increase the viscosity of the blends.

Recently, it has been established that the use of block co-polymers as the toughener can alleviate these processing concerns because the morphology develops spontaneously (self-assembles) upon blending with the uncured precursor, which makes block copolymer modified thermosets attrac-tive for research purposes. As has been reported by several authors, the self-assembly characteristics of block copoly-mers can be maintained in their blends with several homo-polymers.[4] Numerous reports have shown that novel mor-phologies in block copolymers, blends, and solutions can be duplicated in crosslinked systems to give thermosets with in-teresting properties. In this way, block copolymers are widely used as templates for generating nanostructured epoxy or phenolic matrixes with long-range order in both the uncured and cured states.[5–8] For example, Bates et al.[5] have studied methacrylic block copolymer modified epoxy systems and have revealed that these copolymers form nanoscale structures that are typical for dilute blends of asymmetric block copolymers with a solvent selective for the minority block. Like in selective solvents, as the amount of epoxy added to the block copolymer is increased, the blend microstructure evolves from lamellar, to gyroid, to

[a] Dr. Y. Yu, Z. Gao, G. Zhan, L. Li, Prof. S. Li
The Key Laboratory of Molecular Engineering of Polymers
Ministry of Education
and Department of Macromolecular Science
Fudan University, Shanghai, 200433 (China)
Fax: (+86) 21-6564-0293
E-mail: yfyu@fudan.edu.cn
        sjli@fudan.edu.cn

[b] Dr. W. Gan
Department of Macromolecular Materials and Engineering
College of Chemistry and Chemical Engineering
Shanghai University of Engineering Science
Shanghai, 200065 (China)

[c] Prof. J. V. Crivello
Department of Chemistry and Chemical Biology
Rensselaer Polytechnic Institute
1108th Street, Troy, New York 12180 (USA)

cylinders, to body-centered-cubic packed spheres, and ultimately disordered micelles.

However, previous studies[5] have also shown that block copolymers might either lower the heat resistance or increase the viscosity of modified systems when the concentration of copolymers is relatively high. Since liquid-crystalline thermosets[9] have been used to improve the toughness of thermosets without sacrificing other properties, we hoped that polymerizable rod–coil oligomers, which self-assemble in solution and retain their structures during polymerization, might be able to combine the advantages of liquid crystals and copolymers.

It is also well known that self-assembly is a rapid pathway from small molecules to supramolecular, nanometer-sized objects that cannot be synthesized by conventional chemical reactions.[10] This process involves the assembly of discrete ensembles of molecules, supermolecules, and nanoparticles into extended ordered arrays, such as crystals, liquid crystals, and colloids. Block copolymers, especially rod–coil block copolymers, represent a unique class where various hierarchical self-assemblies with different compositions have been observed experimentally.[11] An unprecedented self-organization has been suggested for coil–coil–rod ABC triblock molecules,[12] which can self-assemble into mushroom-shaped nanostructures and further organize into noncentrosymmetric polar monolayer structures. Jenekhe has reported the self-assembly behavior of rod–coil diblock copolymers consisting of poly(phenylquinoline) as the rod block and polystyrene as the coil block.[13] Novel aggregates in the form of hollow spheres, lamellae, hollow cylinders, and vesicles in a solvent selective for the rod segment were observed. These results provide potential applications for new functional materials.

Although block copolymers often self-assemble into nanofibers from well-controlled solutions, it is actually quite difficult to get a nanofiber-reinforced thermosetting network. As reported previously, this is due to technical difficulties arising from the tendency of the growing thermosetting network to expel any kind of inclusions or molecules initially dispersed or solubilized in the precursor mixture.[14]

Except for the blending of hybrid carbon nanotubes[15] and thermotropic liquid crystalline polymers[16] with thermosetting systems, to the best of our knowledge, no report has been published on the use of self-assembled fibers as reinforcing agents in thermosetting systems.

In the present work we report a new method for the creation of fibrils in epoxy networks in situ from an epoxy-terminated ABA rod–coil–rod oligomer bearing aromatic azomethine liquid-crystalline structures. The rod–coil oligomer provides low viscosity before the curing reaction, while the epoxy function, which can be self-polymerized and co-reacted with epoxy precursors, combines with the liquid-crystalline unit to give enhanced thermal properties. During curing of the blends, supramolecular nanoscale columnar structures of the rod–coil oligomer are transformed into polymeric fibrils in the crosslinked epoxy networks.

Results and Discussion

Synthesis and characterization of the rod–coil oligomers: As rod–coil oligomers containing thermosetting mesogens have not been studied as extensively as calamitic liquid-crystalline block copolymers, we decided to synthesize and study a polymerizable ABA rod–coil–rod oligomer. Previous results have shown that a nanostructured system can be obtained by modification of the diglycidyl ether of bisphenol A (DGEBA) with poly(ethylene oxide)(PEO)-based block copolymers.[5] Therefore poly(ethylene oxide), which has good solubility in epoxy resins, was chosen to be the coil unit in our present work, while an aromatic azomethine unit with epoxy end groups was chosen to be the rod unit. The latter is only partly soluble in the uncured epoxy precursor and is present in the liquid-crystalline phase at elevated temperatures.

The dichloro-terminated PEO oligomers were prepared by treatment of the corresponding oligo(ethylene glycol)s with an excess of thionyl chloride in the presence of pyridine and then with 4-hydroxybenzaldehyde to get the aldehyde-terminated PEO oligomers (**2**). As the above synthetic method is well-known, the yield and purity of the products were quite good. Next, the ABA-type, α,ω-modified PEO oligomers were synthesized by first coupling 4-(4-hydroxybenzylideneimino)aniline (**1**) with the aldehyde-terminated PEO oligomers (**2**) and then functionalizing the resultant epoxy (**3**) with a large excess of epichlorohydrin (Scheme 1). The purity of the obtained product (**4**) was checked by TLC, ^{1}H NMR spectroscopy, and GPC. Two rod–coil oligomers were synthesized from PEG 400 and PEG 600 and denoted **LC-400** and **LC-600**, respectively (see Table 3 in the Experimental Section); the molecular weight of their PEO structures is about 400 ($n=9$) and 600 ($n=14$), respectively. **LC-400** and **LC-600** have number molecular weights of about 1130 and 1350, both with a PDI value of 1.2.

Both of the oligomers show mesomorphic phases, and their thermal properties are listed in Table 1. **LC-400** melts into a nematic, liquid-crystalline phase at 128 °C and then transforms into an isotropic liquid at 165 °C, as detected by polarizing optical microscopy (POM). The peak melting temperature (T_m) of the azomethine liquid-crystalline unit is lowered with an increase of PEO unit molecular weight—the transition temperature range is 123–157 °C in **LC-600**. The X-ray diffraction patterns showed only a broad halo during the heating of **LC-400** up to its melting point, which is indicative of the change from the crystalline state to the liquid-crystalline state shown in Figure 1.

As Griffin et al.[17] have reported previously, rod–coil–rod oligomers show only nematic phases. These nematogens have no rigid central core as the two rigid cores are joined by a flexible segment, nevertheless the "center" of the structure is flexible. This flexibility is usually considered deleterious to mesogenic behavior because of the large number of nonlinear geometries the molecule could adopt if the center were flexible. Therefore, an increase of the length of the PEO unit would reduce the tendency to show mesogenic be-
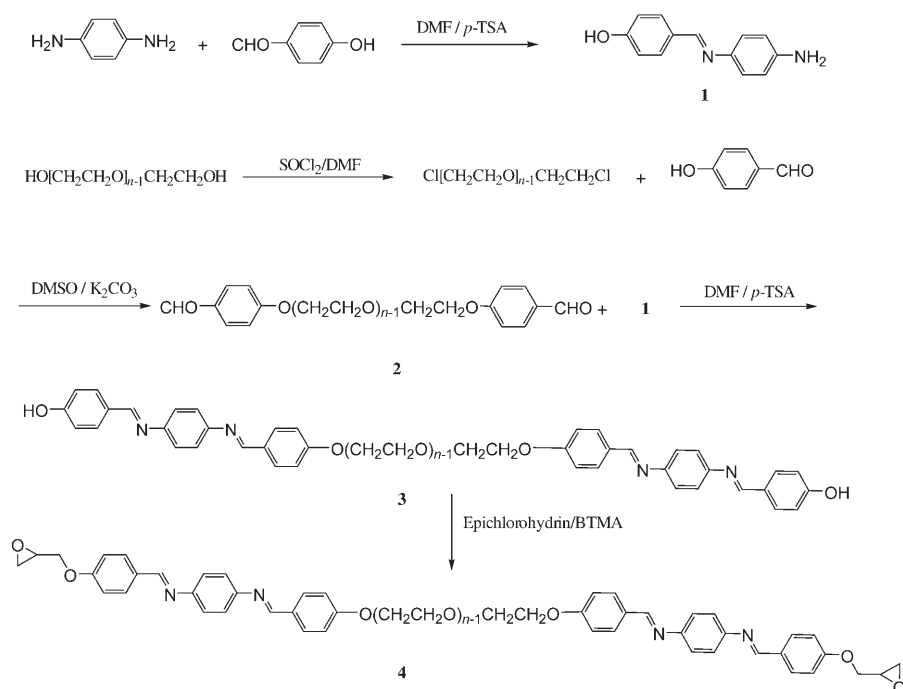
Scheme 1. Synthetic route to the α,ω-modified PEO oligomers ($n = 9$, 14). p-TSA = p-toluenesulfonic acid; BTMA = benzyltrimethylammonium.

columnar bundles and gives rise to the formation of macromolecules with a well-defined shape and size.

The neat oligomer can form columnar (nanorod) structures in both the crystalline and liquid-crystalline states. As this kind of structure is quite stable, it might be possible to preserve this structure during blending with the epoxy precursor to give a nanostructure in the epoxy network.

Morphology of the epoxy blends: The morphology of cured blends was investigated by TM-AFM and SEM. Blending of the rod–coil oligomer with an epoxy precursor and imidazole was performed to get chain-growth-polymerized

Table 1. Characterization of **LC-400** and **LC-600** by differential scanning calorimetry (DSC) and polarized optical microscopy (POM).

Compound	Melting point [°C]		Clear point [°C]	
	DSC	POM	DSC	POM
LC-400	125	128	147	165
LC-600	118	123	141	157

havior, which is why **LC-600** shows a lower transition temperature for both T_m and the clear point than **LC-400**.

To observe the structure directly by AFM, crystalline samples of **LC-400** were prepared by slow cooling of melted samples. As shown in Figure 2, the tapping-mode AFM (TM-AFM) images indicate that **LC-400** self-assembles into a nanoscale, columnar structure with a length of about 10 nm.

For further observation of the mesogenic structure of the oligomer, it was cured in the liquid-crystalline state. A harder, imidazole C11Z was used as anionic initiator as this could provide a quick chain-growth polymerization of the epoxy function. The gel time when curing at 140 °C is less than three minutes, which means that the oligomer remains in the liquid-crystalline state. As shown in Figure 2, the TM-AFM images show organized, discrete bundles of nanoscale, columnar structures about 30 nm in length in the liquid-crystalline phase. When combined with the AFM and XRD observations, these results indicate a preservation of the ordered symmetry and the dimensions of the discrete objects in the LC state after polymerization. Based on the above results, it can be concluded that the polymerization proceeds with retention of the size and shape of the self-assembled
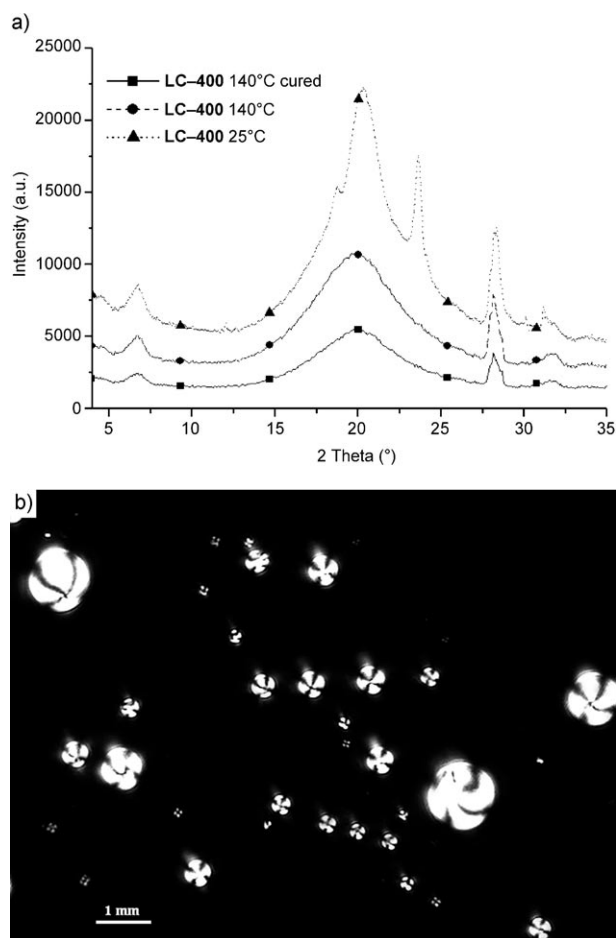
Figure 1. a) X-ray diffraction patterns of **LC-400** in different states and b) the polarizing optical microscopy of **LC-400** at 160 °C.
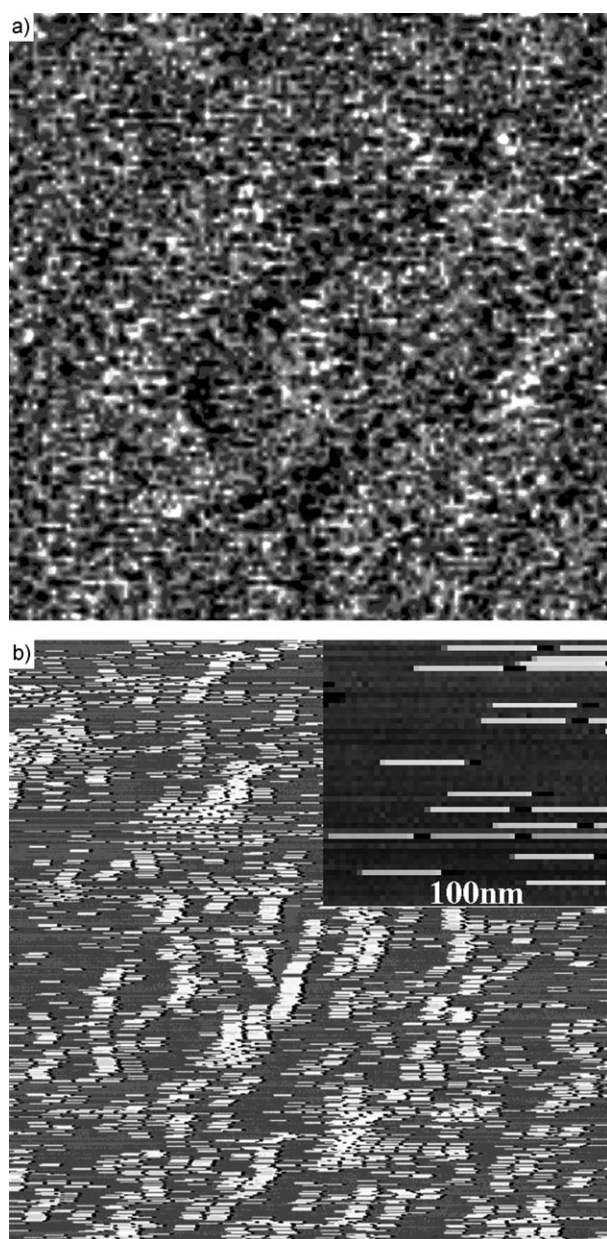
Figure 2. TM-AFM phase image (contrast mode) of **LC-400** at room temperature (image size: 500 nm; z-scale (contrast): 8 nm; scan rate: 1 Hz), and **LC-400** cured with C11Z (4%) at 140°C (image size: 1 mm; z-scale (contrast): 150 nm; scan rate: 1 Hz).

thermoset systems. The samples were cured above the melting point of the oligomer (140°C) or below the melting point of the oligomer (80°C) to evaluate the effect of the liquid-crystalline phase on the morphology of the cured networks.

Remarkably, highly uniform fibrils were observed in the fully cured blend systems by SEM. The SEM images reveal that they are actually fibril-like structures in epoxy blends. As shown in Figure 3, fibrils with a diameter of about 500 nm and longer than 50 mm are observed in all the blends.

The morphology of the fibrils is almost unaffected by a change of curing temperature, that is, in both the crystalline and liquid-crystalline phase. Moreover, the fibrils are formed no matter what weight fraction of rod–coil oligomer is used in the blends. For example, uniform fibrils were observed in the SEM images of **LC-400** 10% systems (Figure 3c), while they were also found in **LC-400** 5% and 20% systems (Figures 3a and 3d).

The quantity and uniformity of the fibrils seems to be affected only by the length of the PEO units of the rod–coil oligomers—the higher the molecular weight of the PEO units, the lower the volume fraction of fibrils observed in the cured sample in the **LC-600** blends.

It should be noted that the blends containing both **LC-400** and **LC-600** oligomers are transparent before curing, which suggests the possibility of microphase separation and nanostructuring. However, the curing reaction results in slightly opaque samples despite this homogeneous dispersion of the oligomers due to their dimensions relative to the wavelength of visible light.

Structure formation process: Previous work has suggested that the ability of diblock copolymers consisting of an epoxy-miscible and an epoxy-immiscible block to form well-defined, ordered and disordered microstructures in thermosetting epoxy resins is not specific to any class of copolymer or thermoset.[5–8] This behavior appears to be highly dependent upon the extent of favorable energetic interactions between the epoxy-miscible block and the cured epoxy network and results in the formation of the ordered and disordered morphologies typical for blends of a block copolymer with a block-selective solvent.

Before curing, the epoxy precursor swells the PEO units, which leads to a morphological behavior similar to those corresponding to nano-ordered homopolymer/block copolymer blends. After curing, the nanostructures are retained and the cure-induced phase transitions occur because of the local expulsion of PEO chains from the epoxy resin matrix.[5–7]

In our case, the morphology of the epoxy blends was studied before and after the curing reaction. TEM images of the rod–coil oligomer/epoxy precursor cast from THF solution at room temperature (25°C) reveal that these oligomers exhibit a behavior in epoxy precursor solution that is very similar to that shown in the previously examined rod–coil oligomer in THF solution. For example, a blend of **LC-400** (20 wt%) in epoxy precursor shows that the rod–coil oligomer forms nanoscale columnar structures typical of its bulk state at room temperature (Figure 4a). However, a significant difference in the structures of the rod–coil oligomer **LC-400** was observed at higher temperatures. As shown in Figure 4b, **LC-400** displays nanoscale fiber structures in a DGEBA/**LC-400** (20%) blend above 73°C, whereas some clusters of **LC-400** are also observed by TEM. Similar phenomena have been explained for hydrogels as being due to a temperature-dependent sol–gel transition in which nonpolymeric hydrogels spontaneously form from small molecules
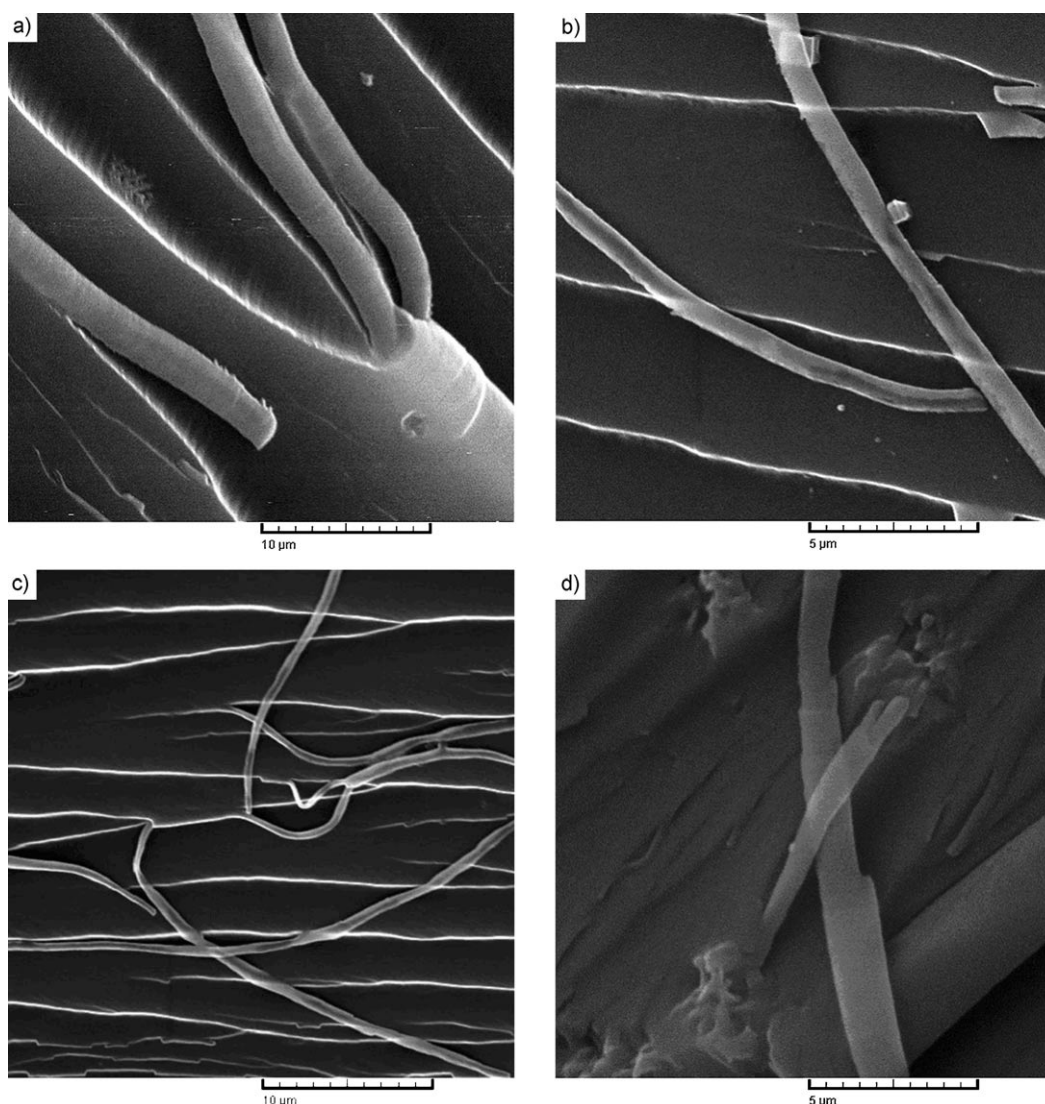
Figure 3. SEM and AFM images of nanofibers formed in DGEBA/**LC-400** (5, 10, or 20%) and **LC-600** (20%)/C11Z cured at 80 or 140°C for 5 h: a) **LC-400**, 5%, 80°C; b) **LC-400**, 5%, 140°C; c) **LC-400**, 10%, 80°C; d) **LC-400**, 20%, 80°C.

and the nanoscale fibers are also transferred from the small molecules due to the dependence of the miscibility on the temperature.[18]
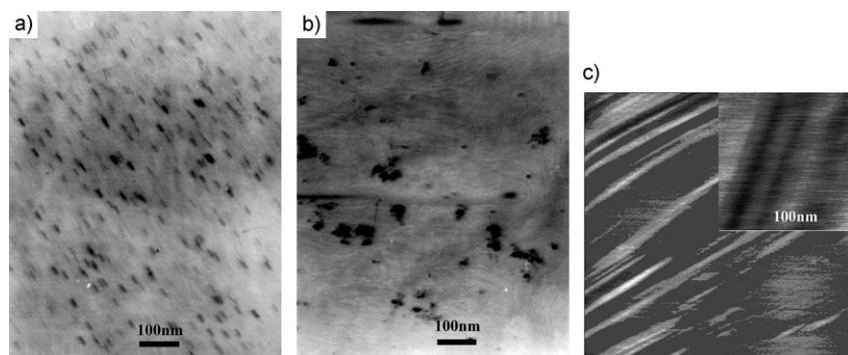

Figure 4. TEM images of DGEBA/**LC-400** (20%) at room temperature (25°C) (a), heated to 80°C (b), and TM-AFM of DGEBA/**LC-400** (20%)/C11Z cured at 80°C for 5 h (c). Image size: 1 mm; z-scale (contrast): 150 nm; scan rate: 1 Hz.

Additionally, in a DGEBA/**LC-400** (20%) blend cured at 80°C in the presence of C11Z, **LC-400** self-assembles into fibril structures (Figure 4c). AFM shows the in situ formation of fibrils during the curing process. These fibrils are in fact bundles of aggregated, regular, oligomeric, nanoscale fibers dispersed in the epoxy matrix with a nanoscopic rod core/PEO shell-like fiber morphologies.

The whole process can be explained by the route shown in Figure 5. As the amorphous PEO and epoxy precursor should be totally miscible,[5] while the azomethine units are insoluble in the epoxy precur-
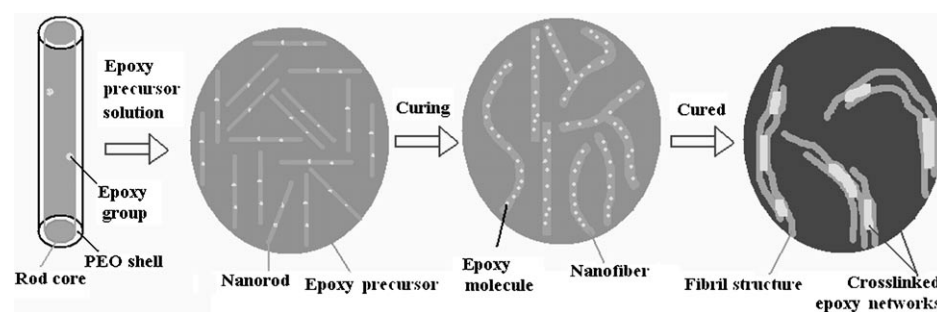
Figure 5. Schematic representation of the self-assembly of rod–coil oligomers in epoxy solution during heating and polymerization.

sor, it can be anticipated that the epoxy precursor should swell the PEO units in these oligomers without dissolving the rod units and lead to an ordered composite before curing. Upon increasing the temperature, the rod unit begins to melt from the crystalline state, which means that some epoxy molecules would diffuse into the ABA rod–coil oligomers and this would enlarge the volume fraction of rod units. The PEO unit cannot therefore maintain the stability of the nanocolumnar structure due to its low volume fraction at this stage. As a result, the nanostructures need to combine to grow into larger structures (nanofibers) in order to get a new balance between the PEO units and rod units in a good solvent.

During the curing process, the polymerization of oligomers themselves and their copolymerization with epoxy molecules would increase the volume fraction and molecular weight of the rod units, and the chain-polymerization of epoxy precursors would change the blends into a ternary system containing growing epoxy chains, epoxy precursors, and polymerizing oligomers. These would decrease the entropy of the blends and the miscibility between the growing epoxy chain and polymerizing oligomers, therefore the structures of rod–coil oligomers would need to aggregate further to keep their stability, which forces the expulsion of the polymerizing oligomers from the epoxy matrix.

It has been reported from both computer simulation and experimental results that when low volume fractions of nanoscale rods are immersed in a binary, phase-separating blend, the rods self-assemble into needlelike, percolating networks.[19] The interconnected network arises through the dynamic interplay of phase-separation between the fluids, preferential adsorption of the minority component onto the mobile rods, and rod–rod repulsion. In our case, the nanoscale fibers of ABA rod–coil oligomers can also be considered as nanoscale rods and the epoxy polymerization induces a phase separation for the same reasons.[19] During phase separation, the strong preferential adsorption drives the phase-separated PEO units to

coat each rod, which means that the rods become strongly confined in the PEO phase. The rods are physically moved by osmotic effects resulting from the phase separation, and the temporal evolution of the fluids "pushes" and "corrals" the rods. Hence, the dynamic coupling between preferential adsorption and phase separation is critical for the formation of the network. Because of the rod–rod repulsion, the high concentrations of rods have a lower free energy when they are arranged end-to-end (beyond the range of the interaction) rather than side-by-side. This end-to-end arrangement deforms the strongly wetting droplets, hence the rod–rod repulsion also plays a crucial role in the formation of the percolating network.

The extension of the rod units makes the fibril structures grow longer and larger, while phase separation of enlarged fibrils from the epoxy matrix further increases the dimension of the fibrils. The combination of these two effects means that the nanoscale fibers of initial rod–coil oligomers quickly grow into fibril structures during the curing reaction.

The imidazole-cured system quickly vitrifies to avoid further phase separation due to polymerization. The curing times for getting 50 % curing conversion are about 13 min at 80 °C and about 3 min at 140 °C for neat epoxy cured by imidazole. At the same time, polymerization of the epoxy endgroup of the rod–coil oligomer results in anchoring of the phase structures in the epoxy matrix, which means that macro-phase separation is avoided due to the quick curing process.

Thermal and mechanical properties: The thermal and mechanical properties of the unmodified and modified polymers are listed in Table 2. As can readily be sees, the incorporation of **LC-400** and **LC-600** sharply increases the glass transition temperature (T_g) of the modified systems compared with the neat epoxy networks, although a further increase of the amount of modifiers decreases T_g slightly. As a higher modulus at the rubbery plateau was observed in the modified systems, the increase in T_g could be attributed to the co-reaction of rod–coil oligomers with the networks,

Table 2. Thermal and tensile properties of selected samples.

Samples[a]	Glass transition temperature [°C]	Tensile modulus [GPa]	Elongation at break [%]	Tensile strength [MPa]
neat epoxy	135	2.44	3.25	50.3
DGEBA/**LC-400** (10 %)	166	2.56	6.13	67.6
DGEBA/**LC-400** (20 %)	160	2.54	6.53	64.2
DGEBA/**LC-600** (10 %)	160	2.47	6.24	57.5
DGEBA/**LC-600** (20 %)	156	2.45	6.58	56.2

[a] All samples were cured at 80 °C for 2 h and post-cured at 150 °C for 4 h.

which might increase the ratio of propagation/termination rates in the anionic chain polymerization and mean that less dangling ends are formed. The PEO unit could also have some effect on the plasticity.

The mechanical properties data show that the tensile strength of all modified samples increases while the length of all modified samples is about twice that of the neat epoxy samples. However, the modulus of the modified blends is comparable to that of the neat epoxy samples. It can therefore be expected that these rod–coil oligomers could be applied for the reinforcement of thermosetting resins and the development of new functional materials.

Conclusion

Polymerizable, liquid-crystalline rod–coil–rod oligomers have been self-assembled into discrete nanorod structures in the liquid-crystalline phase. Crosslinking of the oligomer in the 3D ordered state proceeds with retention of the ordered structure, which leads to the formation of crosslinked objects with a well-defined shape and size. Further blending of the oligomer with an epoxy precursor gives fibril structures in the cured networks with lengths in the micrometer range due to the formation of nanoscale fiber structures by the rod–coil oligomers in the epoxy precursor solution, which suggests that the macromolecular objects are shape-persistent in epoxy precursor solutions as well as in cured networks. Therefore, the polymerization of reactive nanorods within the confined space and formation of fibril structures in epoxy networks offers a novel strategy for the creation of shape-persistent fibril structures which could be applied for the toughening of thermosetting resins and the development of new functional materials.

Experimental Section

Materials: DER331 resin was used as the DGEBA epoxy precursor. 2-Undecylimidazole (trade name C11Z), a white powder with a melting point of 70–74°C, was used as anionic initiator in the epoxy polymerization. Two kinds of commercial poly(ethylene glycol)s, namely PEG 400 and PEG 600, with repeat units of 9 and 14, respectively, were used for

synthesis of the rod–coil oligomers (Table 3). All the other chemicals were provided by Sinopharm Chemical Reagent Co. (China) and purified before use.

4-(4-Hydroxybenzylideneimino)aniline (1): A literature procedure was used for the preparation of this compound.[20] Equimolar amounts of *p*-phenylenediamine and 4-hydroxybenzaldehyde were dissolved in DMF under nitrogen. A few grains of *p*-toluenesulfonic acid were added and the mixture was stirred at 80°C for 4 h. A yellow-orange solid was obtained after precipitation in water. This solid was filtered and washed with methanol/water (50:50, v/v), then stirred twice with fresh methanol/water (50:50, v/v) and filtered off. The orange-colored product was vacuum-dried at 60°C for 18 h. M.p. 241°C (DSC). ^{1}H NMR ([D$_6$]DMSO): $\delta = 8.45$ (s, 1H; CH=N), 8.0–6.6 (m, 12H; aromatic), 4.25 ppm (br.s, 2H; NH$_2$).
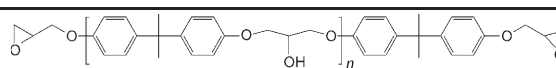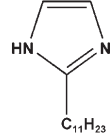
Aldehyde-terminated PEG ethers (2): A procedure described for the preparation of 1,4-dichlorobutane[21] was used for the preparation of the PEG dichloride. The glycols HO(-CH$_2$-CH$_2$-O)$_n$-H (1 mol) and dry pyridine (12.4 g, 0.1048 mol) were introduced into a flask fitted with a condenser. Thionyl chloride (4 mol) was added dropwise to this mixture over 2.5 h whilst stirring and cooling in an ice bath. Stirring was continued for 24 h at room temperature and this was followed by refluxing for 4.5 h. The reaction mixture was then poured into an ice–water mixture. The organic layer was separated and the aqueous layer was extracted several times with ethyl acetate. An aqueous (10%) solution of NaHCO$_3$ was then added to the combined organic layers. The organic layer was separated, washed with water, dried with anhydrous MgSO$_4$, and filtered. The solvent was removed from the filtrate, and the residue was subjected to vacuum distillation to yield the α,ω-dichloropoly(ethylene oxide)s (yield: 70%) as pale-yellow liquids.

The above dichloride (0.1 mol), K$_2$CO$_3$ (14.0 g, 0.25 mol), 4-hydroxybenzaldehyde (30.5 g, 0.25 mol), and 250 mL of dry DMSO were introduced into a flask equipped with a mechanical stirrer and a gas inlet. The reaction mixture was stirred and heated (130°C) under nitrogen for 24 h. It was then poured into an ice–water mixture. The organic layer was separated and the aqueous layer was extracted several times with ethyl acetate. The organic layer was separated and extracted with water to remove the water-soluble PEG from the organic layer. The solution was dried with anhydrous MgSO$_4$ and filtered. The solvent was then evaporated and the crude product was purified by column chromatography (silica gel; eluent: hexane/ethyl acetate, 3/1) to give compound **2** as a pale yellow oil (yield 70%).

Aldehyde-terminated PEG 400 ether: ^{1}H NMR (CDCl$_3$): $\delta = 9.96$–9.92 (m, 2H; CH=O), 7.83–7.81 (m, 4H; aromatic), 7.12–7.09 (m, 4H; aromatic), 4.18 (br.s, 4H; PhO-CH$_2$), 3.89 (br.s, 4H; PhO-CH$_2$-CH$_2$), 3.71–3.63 ppm (m; O-CH$_2$-CH$_2$-O).

Aldehyde-terminated PEG 600 ether: ^{1}H NMR (CDCl$_3$): $\delta = 9.96$–9.92 (m, 2H; CH=O), 7.83–7.81 (m, 4H; aromatic), 7.12–7.09 (m, 4H; aromatic), 4.18 (br.s, 4H; PhO-CH$_2$), 3.89 (br.s, 4H; PhO-CH$_2$-CH$_2$), 3.71–3.63 ppm (m; O-CH$_2$-CH$_2$-O).

Table 3. Characteristics of the epoxy precursor, initiator, and PEOs used in this work.

Name	Designation	Chemical structure	M_n	Supplier
diglycidyl ether of bisphenol A	DGEBA		186–192 g equiv^{-1}	Dow Chemical Co.
2-undecylimidazole	C11Z		222 g mol^{-1}	Shikoku Chemical Co. (Japan)
poly(ethylene glycol)s	PEG 400 ($n=9$)[a]	HO[CH$_2$CH$_2$O]$_{n-1}$CH$_2$CH$_2$OH	414 g mol^{-1}	Sinopharm Chemical Reagent Co. (China)
poly(ethylene glycol)s	PEG 600 ($n=14$)[a]	HO[CH$_2$CH$_2$O]$_{n-1}$CH$_2$CH$_2$OH	634 g mol^{-1}	Sinopharm Chemical Reagent Co. (China)

[a] PDI (polydispersity index, M_w/M_n) value of 1.1. (as determined by GPC).

Bis-Schiff base of PEG ethers (3): Equimolar amounts of **1** and the aldehyde-terminated PEG ethers **2** were dissolved in DMF with a few drops of glacial acetic acid and the mixture stirred whilst heating at 60°C for 15 min. The temperature was then raised to 90°C and the stirring continued for 4 h. After cooling, the reaction mixture was poured into water, the organic layer separated, and the aqueous layer extracted several times with ethyl acetate. The organic solution was washed with water and brine and dried with anhydrous $MgSO_4$. The solvent was evaporated, and the crude product was purified by column chromatography (silica gel; eluent: hexane/ethyl acetate, 2/1) to give compound **3** as a yellow, wax-like solid (yield: 90%).

Bis-Schiff base of PEG 400 ether: ^1H NMR ($CDCl_3$): $\delta = 7.63$–7.58 (m, 4H; aromatic), 7.54–7.51 (m, 4H; aromatic), 7.41–6.38 (m, 8H; aromatic), 6.95–6.82 (m, 8H; aromatic), 5.08 (s, 2H; PhOH), 4.19 (br. s, 4H; PhO-CH_2), 3.91 (br. s, 4H; PhO-CH_2-CH_2), 3.71–3.63 ppm (m; O-CH_2-CH_2-O).

Bis-Schiff base of PEG 600 ether: ^1H NMR ($CDCl_3$): $\delta = 7.63$–7.58 (m, 4H; aromatic), 7.54–7.51 (m, 4H; aromatic), 7.41–6.38 (m, 8H; aromatic), 6.95–6.82 (m, 8H; aromatic), 5.08 (s, 2H; PhOH), 4.19 (br. s, 4H; PhO-CH_2), 3.91 (br. s, 4H; PhO-CH_2-CH_2), 3.71–3.63 ppm (m; O-CH_2-CH_2-O).

α,ω-Modified PEO rod–coil oligomers (4): Compound **3** (0.05 mol) was dissolved in 90 mL of epichlorohydrin(molar ratio: 40:1). After heating at 110°C and stirring for 1 h, the solution became clear and benzyltrimethylammonium(BTMA) was added as catalyst. The mixture was then refluxed for another 2 h. Epichlorohydrin was removed by distillation and the residue was purified by column chromatography (silica gel; eluent: hexane/ethyl acetate, 2/1) to give **4** in 95% yield as a yellow solid.

LC-400: ^1H NMR ($CDCl_3$): $\delta = 8.42$ (s, 4H; CH=N), 7.84–7.83 (m, 8H; aromatic), 7.26–7.24 (m, 8H; aromatic), 7.00–6.98 (m, 8H; aromatic), 4.25, 4.02 (m, 4H; epoxy-CH_2-O), 4.19 (br. s, 4H; PhO-CH_2), 3.88 (br. s, 4H; PhO-CH_2-CH_2), 3.72–3.64 (m; O-CH_2-CH_2-O), 3.37 (s, 2H; CH in epoxy ring), 2.85, 2.79 ppm (m, 4H; CH_2 in epoxy).

LC-600: ^1H NMR ($CDCl_3$): $\delta = 8.42$ (s, 4H; CH=N), 7.84–7.83 (m, 8H; aromatic), 7.26–7.24 (m, 8H; aromatic), 7.06–6.98 (m, 8H; aromatic), 4.25, 4.02 (m, 4H; epoxy-CH_2-O), 4.19 (br. s, 4H; PhO-CH_2), 3.88 (br. s, 4H; PhO-CH_2-CH_2), 3.72–3.64 (m; O-CH_2-CH_2-O), 3.37 (s, 2H; CH in epoxy ring), 2.85, 2.79 ppm (m, 4H; CH_2 in epoxy).

Measurements: ^1H NMR spectra were recorded with a Bruker DMX 500 spectrometer (500 MHz). The polydispersities of the samples were measured with a Perkin–Elmer S-250 gel permeation chromatograph (GPC) equipped with a Perkin–Elmer LC-235 UV detector set at 245 nm and an LC-30 RI refractive index detector, and using three Waters Styragel columns (HR 2, HR 4, and HR 5E), whose molecular weight detection range is 500–20000, 5000–500000 and 2000–4000000, respectively.

XRD experiments were performed with a Philips X'pert MPD Pro X-ray diffractometer. The thermal properties of the polymer samples were determined with a Perkin–Elmer Pyris 1 differential scanning calorimeter equipped with a liquid nitrogen cooling accessory. A 3–6-mg sample of the purified material was placed on an aluminum pan and measured against another empty pan as a reference.

Polarized light microscopy (PLM) experiments were performed with an Olympus BX51P microscope equipped with an Instec HCS410 hot stage. Atomic force microscopy (AFM) was performed with a Nanoscope IV scanning microscope (controller, Veeco Metrology Group). The experiments were performed in the soft tapping mode and the height and phase images were obtained under ambient conditions in dry air (RH $\approx 20\%$)with typical scan speeds of 0.5–1 lines per second.

Transmission electronic microscopy (TEM) was performed with a JEM-1200EX TEM; samples of rod–coil oligomers and uncured blends were prepared in THF solution. Both AFM and TEM samples of cured blends were prepared with an ultramicrotome (Leica Ultracut R) equipped with a diamond knife. The morphologies of the isothermally cured blends were observed under a scanning electron microscope (Tescan TS 5163 MM) for samples fractured in liquid nitrogen. All samples were coated with gold and mounted on copper mounts.

The dynamic mechanical properties were determined in the dual-cantilever bending mode between room temperature and 400°C for rectangular polymer samples of approximate dimensions $1 \times 3 \times 30$ mm^3 using a Netzsch DMA 242 apparatus. The measuring frequency was 1 Hz, the sample displacement was 3 mm, and the heating rate was 10°C min^{-1}. The mechanical properties of the samples were recorded with an Instron-8500 universal tester according to China State Standard GB 1040-79.

Sample preparation: Crystalline samples of rod–coil oligomer **LC-400** were prepared by the slow cooling of melted samples at a rate of approximately 0.1°C min^{-1} on a silicon wafer to room temperature. For the polymerization of the ABA rod–coil oligomers, **LC-400** was dissolved in THF with 4% of 2-undecylimidazole (C11Z) and, after removal of the solvent, the sample was cured in the liquid-crystalline state at 140°C under nitrogen for 5 h. Rod–coil oligomers (**LC-400** or **LC-600**) with the epoxy precursor were prepared by dissolving the oligomer (5%, 10%, and 20% by weight) in the epoxy precursor at elevated temperature and adding 4% of imidazole C11Z to the blend to yield an optically homogeneous mixture.

[1] a) H. Zhang, L. A. Berglund, *Polym. Eng. Sci.* **1993**, *33*, 100–107; b) H. Hsich, *Polym. Eng. Sci.* **1990**, *30*, 493–510; c) H. S. Lee, T. Kyu, *Macromolecules* **1990**, *23*, 459–464.

[2] a) C. B. Bucknall, C. M. Gomez, I. Quintard, *Polymer* **1994**, *35*, 353–359; b) B. G. Min, J. H. Hodgkin, Z. H. Stachurski, *J. Appl. Polym. Sci.* **1993**, *50*, 1065–1073; c) G. S. Bennett, R. J. Farris, S. A. Thompson, *Polymer* **1991**, *32*, 1633–1641; d) C. C. Riccardi, J. Borrajo, R. J. J. Williams, E. Girard-Reydet, H. Sautereau, J. P. Pascault, *J. Polym. Sci., Part B: Polym. Phys.* **1996**, *34*, 349–356; e) A. Bonnet, J. P. Pascault, H. Sautereau, M. Taha, Y. Camberlin, *Macromolecules* **1999**, *32*, 8517–8523; f) Y. F. Yu, M. H. Wang, W. J. Gan, S. J. Li, *J. Phys. Chem. B* **2004**, *108*, 6208–6215.

[3] a) G. Levita, A. Marchetti, A. Lazzeri, *Makromol. Chem. Macromol. Symp.* **1991**, *41*, 179–194; b) H. J. Sue, *J. Mater. Sci.* **1992**, *27*, 3098–3107; c) J. Choi, A. F. Yee, R. M. Laine, *Macromolecules* **2004**, *37*, 3267–3276.

[4] a) M. W. Matsen, *Macromolecules* **1995**, *28*, 5765–5773; b) *Polymer Blends* (Eds.: D. R. Paul, S. Newman), Academic Press, New York, **1978**, Vol. 1; c) M. Xanthos, S. S. Dagli, *Polym. Eng. Sci.* **1991**, *31*, 929–935; d) C. Auschra, R. Stadler, *Macromolecules* **1993**, *26*, 6364–6367; e) C. Koning, M. V. Duin, C. Pagnoulle, R. Jerome, *Prog. Polym. Sci.* **1998**, *23*, 707–757.

[5] a) R. B. Grubbs, J. M. Dean, F. S. Bates, *Macromolecules* **2001**, *34*, 8593–8595; b) M. A. Hillmyer, P. M. Lipic, D. A. Hadjuk, K. Almdal, F. S. Bates, *J. Am. Chem. Soc.* **1997**, *119*, 2749–2750; c) P. M. Lipic, F. S. Bates, M. A. Hillmyer, *J. Am. Chem. Soc.* **1998**, *120*, 8963–8970; d) J. M. Dean, P. M. Lipic, R. B. Grubbs, R. F. Cook, F. S. Bates, *J. Polym. Sci., Part B: Polym. Phys.* **2001**, *39*, 2996–3010; e) R. B. Grubbs, J. M. Dean, M. E. Broz, F. S. Bates, *Macromolecules* **2000**, *33*, 9522–9534.

[6] J. Mijovic, M. Shen, J. W. Sy, I. Mondragon, *Macromolecules* **2000**, *33*, 5235–5244.

[7] a) Q. Guo, R. Thomann, W. Gronski, T. Thurn-Albrecht, *Macromolecules* **2002**, *35*, 3133–3144; b) Q. Guo, R. Thomann, W. Gronski, R. Staneva, R. Ivanova, B. Stuhn, *Macromolecules* **2003**, *36*, 3635–3645.

[8] a) S. Ritzenthaler, F. Court, L. David, E. Girard-Reydet, L. Leibler, J. P. Pascault, *Macromolecules* **2002**, *35*, 6245–6254; b) S. Ritzenthaler, F. Court, L. David, E. Girard-Reydet, L. Leibler, J. P. Pascault, *Macromolecules* **2003**, *36*, 118–126; c) V. Rebizant, V. Abetz, F.

Tournilhac, F. Court, L. Leibler, *Macromolecules* **2003**, *36*, 9889–9896; d) V. Rebizant, A. S. Venet, F. Tournilhac, E. Girard-Reydet, C. Navarro, J. P. Pascault, L. Leibler, *Macromolecules* **2004**, *37*, 8017–8027.

[9] a) G. G. Barclay, C. K. Ober, *Prog. Polym. Sci.* **1993**, *18*, 899–945; b) S. Atsushi, K. O. Christopher, *Prog. Polym. Sci.* **1997**, *22*, 975–1000; c) A. P. Melissaris, M. H. Litt, *Macromolecules* **1994**, *27*, 2675–2684; d) S. Cho, E. P. Douglas, *Macromolecules* **2002**, *35*, 4550–4552; e) C. Carfagna, E. Amendola, M. Giamberini, *Comput. Struct.* **1994**, *27*, 37–43; f) C. B. Tan, H. Sun, B. M. Fung, B. P. Grady, *Macromolecules* **2000**, *33*, 6249–6254.

[10] a) S. I. Stupp, V. LeBonheur, K. Walker, L. S. Li, K. E. Huggins, M. Keser, A. Amstutz, *Science* **1997**, *276*, 384–389; b) S. C. Zimmerman, F. Zeng, D. E. C. Reichert, S. V. Kolotuchin, *Science* **1996**, *271*, 1095–1098; c) J. C. M. van Hest, D. A. P. Delnoye, M. W. P. L. Baars, M. H. P. van Genderen, E. W. Meijer, *Science* **1995**, *268*, 1592–1595; d) V. Percec, G. Johansson, G. Ungar, J. Zhou, *J. Am. Chem. Soc.* **1996**, *118*, 9855–9866.

[11] a) M. Lee, B. K. Cho, W. C. Zin, *Chem. Rev.* **2001**, *101*, 3869–3892; b) C. Y. Li, K. K. Tenneti, D. Zhang, H. L. Zhang, X. H. Wan, E. Q. Chen, Q. F. Zhou, A. O. Carlos, S. Igos, B. S. Hsiao, *Macromolecules* **2004**, *37*, 2854–2860; c) S. V. Arehart, C. Pugh, *J. Am. Chem. Soc.* **1997**, *119*, 3027–3037.

[12] a) M. U. Pralle, K. Urayama, G. N. Tew, D. Neher, G. Wegner, S. I. Stupp, *Angew. Chem.* **2000**, *112*, 1546–1549; *Angew. Chem. Int. Ed.* **2000**, *39*, 1486–1489; b) E. R. Zubarev, M. U. Pralle, L. Li, S. I. Stupp, *Science* **1999**, *283*, 523–526.

[13] a) S. A. Jenekhe, X. L. Chen, *Science* **1998**, *279*, 1903–1907; b) X. L. Chen, S. A. Jenekhe, *Langmuir* **1999**, *15*, 8007–8017.

[14] A.-V. Ruzette, L. Leibler, *Nat. Mater.* **2005**, *4*, 19–31.

[15] a) L. S. Schadler, S. C. Giannaris, P. M. Ajayan, *Appl. Phys. Lett.* **1998**, *73*, 3842–3844; b) K. T. Lau, S. Q. Shi, *Carbon* **2002**, *40*, 2965–2968; c) S. R. Wang, Z. Y. Liang, T. Liu, B. Wang, C. Zhang, *Nanotechnology* **2006**, *17*, 1551–1557.

[16] a) S. Barrau, P. Demont, E. Perez, A. Peigney, C. Laurent, C. Lacabanne, *Macromolecules* **2003**, *36*, 9678–9680; b) Y. Breton, G. Désarmot, J. P. Salvetat, S. Delpeux, C. Sinturel, F. Béguin, S. Bonnamy, *Carbon* **2004**, *42*, 1027–1030.

[17] A. C. Griffin, T. R. Britt, *J. Am. Chem. Soc.* **1981**, *103*, 4957–4959.

[18] a) J.-H. Fuhrhop, C. Boettcher, *J. Am. Chem. Soc.* **1990**, *112*, 1768–1776; b) M. Jokic, J. Makarevic′, M. Zÿinic, *J. Chem. Soc. Chem. Commun.* **1995**, 1723–1725; c) L. A. Estroff, A. D. Hamilton, *Angew. Chem.* **2000**, *112*, 3589–3592; *Angew. Chem. Int. Ed.* **2000**, *39*, 3447–3450; d) C. Marmillon, F. Gauffre, T. Gulik-Krzywicki, C. Loup, A.-M. Caminade, E. Rump, *Angew. Chem.* **2001**, *113*, 2696–2699; *Angew. Chem. Int. Ed.* **2001**, *40*, 2626–2629;.

[19] a) G. W. Peng, F. Qiu, V. V. Ginzburg, D. Jasnow, A. C. Balazs, *Science* **2000**, *288*, 1802–1804; b) K. H. Wu, S. Y. Lu, *Macromol. Rapid Commun.* **2006**, *27*, 424–429; c) I. Szleifer, R. Yerushalmi-Rozen, *Polymer* **2005**, *46*, 7803–7818; d) G. J. van Maanen, S. L. Seeley, M. D. Capracotta, S. A. White, R. R. Bukovnik, J. Hartmann, J. D. Martin, R. J. Spontak, *Langmuir* **2005**, *21*, 3106–3115.

[20] V. Cozan, E. Avram, *Eur. Polym. J.* **2003**, *39*, 107–114.

[21] a) *Vogel's Textbook of Practical Organic Chemistry*, Longman, New York, **1978**, p. 385; b) B.-A. Feit, B. Halak, *J. Polym. Sci. Part A: Polym. Chem.* **2002**, *40*, 2171–2183.